Published in final edited form as:
Cancer Res. 2009 January 15; 69(2): 678–686. doi:10.1158/0008-5472.CAN-08-3980.

Tgfbr1 haploinsufficiency is a potent modifier of colorectal cancer development

Qinghua Zeng[1,*], **Sharbani Phukan**[2,3,*], **Yanfei Xu**[2,3], **Maureen Sadim**[2,3], **Diana S. Rosman**[2,3], **Michael Pennison**[1], **Jie Liao**[3,4], **Meng Zhang**[3,4], **Guang-Yu Yang**[3,4], **Chiang-Ching Huang**[3,5], **Laura Valle**[6], **Antonio Di Cristofano**[7], **Albert de la Chapelle**[6], and **Boris Pasche**[1]

[1]Division of Hematology/Oncology, Department of Medicine and Comprehensive Cancer Center, The University of Alabama at Birmingham, Birmingham, AL 35294

[2]Cancer Genetics Program, Division of Hematology/Oncology, Department of Medicine, Northwestern University, Chicago, IL 60611

[3]Robert H. Lurie Comprehensive Cancer Center, The Feinberg School of Medicine, Northwestern University, Chicago, IL 60611

[4]Department of Pathology, Northwestern University, Chicago, IL 60611

[5]Department of Preventive Medicine, Northwestern University, Chicago, IL 60611

[6]Human Cancer Genetics Program, The Ohio State University Comprehensive Cancer Center, Columbus, OH 43210

[7]Department of Developmental and Molecular Biology, Albert Einstein College of Medicine, Bronx, NY 10461

Abstract

TGF-β signaling is frequently altered in colorectal cancer. Using a novel model of mice heterozygous for a targeted null mutation of *Tgfbr1* crossed with $Apc^{Min/+}$ mice, we show that $Apc^{Min/+}$;$Tgfbr1^{+/-}$ mice develop twice as many intestinal tumors as $Apc^{Min/+}$;$Tgfbr1^{+/+}$ mice as well as adenocarcinoma of the colon, without loss of heterozygosity at the *Tgfbr1* locus. Decreased Smad2 and Smad3 phosphorylation and increased cellular proliferation are observed in the colonic epithelium crypts of $Apc^{Min/+}$;$Tgfbr1^{+/-}$ mice. Smad-mediated TGF-β signaling is preserved in both $Apc^{Min/+}$;$Tgfbr1^{+/+}$ and $Apc^{Min/+}$;$Tgfbr1^{+/-}$ intestinal tumors but cyclin D1 expression and cellular proliferation are significantly higher in $Apc^{Min/+}$;$Tgfbr1^{+/-}$ tumors. These results show that reduced Tgfbr1-mediated TGF-β signaling significantly enhances colorectal cancer development and results in increased tumor cell proliferation. These findings provide a plausible molecular mechanism for colorectal cancer development in individuals with constitutively altered TGFBR1 expression, a recently identified common form of human colorectal cancer.

Keywords

Tgfbr1; Transforming growth factor beta; haploinsufficiency; colon cancer; SMAD

Correspondence to:, Boris Pasche, M.D., Ph.D., Division of Hematology/Oncology, Department of Medicine, The University of Alabama at Birmingham, 1802 6th Ave South, NP 2566, Birmingham, AL 35294-3300, Phone: 205-934-9591, Fax: 205-975-2669, Email: E-mail: Boris.Pasche@ccc.uab.edu.
*These authors contributed equally to this work

Introduction

There is growing evidence that constitutive as well as somatically acquired alterations in TGF-β signaling are associated with colorectal cancer risk and disease progression. Germline mutations of the *SMAD4* and *BMPR1A* genes are associated with juvenile polyposis (1) and common and functionally-relevant alleles of *SMAD7* influence colorectal cancer risk (2). There is also evidence that loss of SMAD signaling in human colorectal cancer is associated with advanced disease and poor prognosis (3). Analysis of 13,023 genes in human colorectal cancers has shown that four of the 69 most frequently mutated genes are constitutive elements of the TGF-β signaling pathway: *TGFBR2*, *SMAD2*, *SMAD3* and *SMAD4* (4).

The central role of impaired TGF-β and Bone Morphogenic Protein (BMP) signaling in colon cancer development and progression was first demonstrated in animal experiments by the use of cis-$Apc^{+/\Delta 716}$ $Smad4^{+/-}$ compound mutant mice (5). In the compound mutant mice, complete loss of Smad4-dependent TGF-β signaling causes intestinal adenomas to develop into adenocarcinomas. Other animal experiments have shown that complete loss of *Tgfbr2* in intestinal epithelial cells promotes the invasion and malignant transformation of tumors (6). Complete *Smad3* deficiency promotes tumorigenesis in the distal colon of $Apc^{Min/+}$ mice (7) and complete loss of Smad4-dependent signaling in T cells has been shown to increase spontaneous gastrointestinal tumorigenesis (8). While increased gastrointestinal tumor susceptibility has not yet been reported in $Tgfbr1^{+/-}$, $Tgfbr2^{+/-}$, $Smad2^{+/-}$ or $Smad3^{+/-}$ mice, $Smad4^{+/-}$ mice are predisposed to the development of late-onset polyps in the upper gastrointestinal tract (9–11). Whether haploinsufficiency of any of the TGF-β genes contributes to colorectal cancer development is unknown.

We have previously identified *TGFBR1**6A, which encodes a common human TGFBR1 variant (12) and transduces TGF-β signaling less effectively than TGFBR1 (13;14). Cancer risk is higher for *TGFBR1**6A homozygotes than for *TGFBR1**6A heterozygotes among patients with hereditary colorectal cancer and no evidence of mismatch repair deficiency, which suggests that constitutively decreased TGF-β signaling modifies cancer risk (15;16). These findings led us to hypothesize that decreased Tgfbr1-mediated TGF-β signaling may be a modifier of cancer susceptibility (17). Here we report on a novel $Tgfbr1^{+/-}$ mouse model generated to test the hypothesis that constitutively decreased Tgfbr1 signaling is causally involved in colorectal cancer development. When $Tgfbr1^{+/-}$ mice in mixed 129Svlm/C57BL/6 background were crossed with $Apc^{Min/+}$ mice, a significantly higher number of tumors was observed in $Apc^{Min/+}$; $Tgfbr1^{+/-}$ mice than in $Apc^{Min/+}$; $Tgfbr1^{+/+}$ mice. These findings confirmed our hypothesis and prompted us to investigate the relevance of these findings in humans. We considered *TGFBR1* to be a notable candidate for a gene that, when mutated, causes predisposition to CRC or acts as a modifier of other genes resulting in a predisposition. This led to the discovery that 12% of patients with colorectal cancer and 1.5% of healthy controls have evidence of germline decreased TGFBR1 expression (18). Thus, this novel phenotype likely accounts for a significant proportion of human colorectal cancers (18). This report describes new mechanistic insights into the role of Tgfbr1 signaling in colorectal cancer development both in mixed 129Svlm/C57BL/6 and pure C57BL/6 backgrounds with significant implications for human colorectal cancer.

Materials and Methods

Generation of a targeted Tgfbr1 mouse Model

Using mouse genomic DNA as a template, we designed *Tgfbr1* primers amplifying a 491 base pair fragment spanning from position 27 (exon 1) to position 517 (exon 3). Using an isogenic 129SvIm genomic library (Stratagene), we picked several clones, grew them and excised the insert through NotI cleavage. Two overlapping clones were obtained that spanned this genomic

region. We found a NotI site 5-bp downstream of the ATG start codon. The targeting vector has been designed to insert the Neo cassette into the Not I site, thus interrupting the *Tgfbr1* open reading frame and removing 1.1kb mouse genomic sequence immediately upstream of this Not I site. Following transfection and selection of 129SvIm embryonic stem (ES) cells, KO clones were karyotyped and injected into C57BL/6 blastocysts. Germline transmission from the resulting chimeras was obtained and a colony established. F3 $Tgfbr1^{+/-}$ mice were backcrossed into the C57BL6/J background using speed congenics markers. Briefly, a minimum of 8 $Tgfbr1^{+/-}$ animals from each generation of backcrossing were genotyped for 152 markers by the Jackson Laboratory (Bar Harbor, ME) (See Supplementary Table 1). Mice with the highest percentage of the host genome were used to backcross to the host for the next generation. Two fully congenic F6 males (99.9% C57BL6/J) were confirmed using a full genome wide panel of 150 SNP markers (Jackson laboratory, Bar Harbor, ME). These two males were crossed with C57BL6/J females to obtain pure $Tgfbr1^{+/-}$ mice in the C57BL6/J background.

$Tgfbr1^{+/-}$ genotype was confirmed by PCR analysis using the following set of 3 primers: 5'-AGACCCCAGCTCTTAGCCCCCA -3', 5'-GAGACGCTCCACCCACCTTCCC-3', and 5'-GAAGCTGACTCTAGAGGATCCC-3'. PCR amplification results in 2 bands in $Tgfbr1^{+/-}$ mice (240 bp and 314 bp, corresponding to the knocked-out and WT *Tgfbr1* allele, respectively) (See Figure 1B). Pure $Tgfbr1^{+/-}$ female mice in C57BL/6J were mated with C57BL/6J $Apc^{Min/+}$ male mice to generate pure C57BL6/J animals harboring $Tgfbr1^{+/-}$ or $Tgfbr1^{+/+}$. The $Apc^{Min/+}$ locus was detected by PCR using the following primers: 5'-TTCCACTTTGGCATAAGGC-3', 5'-TTCTGAGAAAGACAGAAGTTA-3'. PCR amplification results in a band of 340 bp (Supplementary Fig. 1).

Histopathology of intestinal polyps and polyp scoring

The number and size of polyps were scored by two examiners. Tissue specimens were prepared according to standard protocols. Polyps from seven randomized mice from each group were sectioned, stained with H&E, to differentiate tumors from lymphoid aggregates.

Mouse embryonic fibroblasts

Mouse embryonic fibroblasts (MEFs) were collected at embryonic day 12.5 according to standard protocol (19) and cultured in DMEM (Invitrogen, Carlsbad, CA) supplemented with 10% FBS (Hyclone, Logan, UT), 2 mM L-glutamine, and 100 units/ml penicillin/streptomycin (20).

Spontaneous Cell Proliferation Assay

MEFs were seeded in normal growth medium at a concentration of 5×10^4 cells per well in 6 well plates on day 0. Cell number was determined by trypsinizing and counting cells on day 1, 2 and 3.

TGF-β-mediated Cell Proliferation Assays

TGF-β-mediated cell growth inhibition was assessed by ^{3}H-thymidine incorporation assays as previously described (21).

Luciferase assays

The 3TP-Lux and SBE4-Lux reporter constructs were gifts of Dr. Joan Massagué (Sloan-Kettering) and Dr. Bert Vogelstein (Hopkins). The experiments were performed as described before (22).

Immunoblotting and Immunohistochemistry

Nuclear extracts from mouse embryonic fibroblast were obtained using a NE-PER nuclear and cytoplasmic extraction kit (Thermo Fisher Scientific, Inc., Rockford, IL, cat # 78833). Cell lysates were collected in lysis buffer (TNT buffer (10 mM Tris pH 8.0, 1% Triton X-100, 1 mM EDTA, 150 mM NaCl), supplemented with Phosphatase Inhibitor Cocktails 1 and 2, and Protease Inhibitor Cocktail (Sigma, St. Louis, MO)), and centrifuged at 14000xg for 15 min. above. All lysates were separated by SDS-PAGE gels (Invitrogen, Carlsbad, CA), and transferred onto nitrocellulose (GE Healthcare, Buckinghamshire, England). Immunoblotting was done using the following antibodies: rabbit anti-TGFBR1 (sc-398), anti-cyclin D1 (sc-753), anti-TGFBR2 (sc- 220), anti-p15 (sc-613), anti-Cdk4 (sc-260), mouse anti-Cdk2 (sc-6248), anti-Cdk6 (sc-56282), anti-p21 (sc-6246), anti-p27 (sc-1641), and anti-Histone 1 (sc-8030) (Santa Cruz Biotechnology, Santa Cruz, CA); rabbit anti-pSmad2 (cat #3101) (Cell Signaling Technology, Boston, MA); rabbit anti-pSmad3 was a gift from Dr. Koichi Matsuzaki, Kanzai Medical University, Osaka, Japan. Signal detection was measured by SuperSignal West Femto Chemiluminescent Substrate (Thermo Fisher Scientific, Inc., Rockford, IL). Films were scanned and densitometry was performed using Fujifilm LAS-3000 (Fuji Medical System, USA).

Immunohistochemistry

was performed with the Dako EnVision System (Carpinteria, CA) Percentage of positively stained cells was determined by assessing the number of strongly positive stained cells out of the total number of cells in a field. Five representative fields in 3 different samples were assessed.

Loss of Heterozygosity (LOH) Analyses

SNaPshot methodology (PE Applied Biosystems, Foster City, CA) was used to identify each allele, and to detect loss of heterozygosity (LOH) in tumor DNA.

Statistical Analysis

Data were analyzed by Student's t-test and are expressed as mean ± S.E.M. p values < 0.05 were considered significant. All tests were two-tailed. Data were transformed in logarithm scale when normality assumption was violated. One-way ANOVA was used for the analysis of Tgfbr1 expression in various tissues (Figure 1C). Chi-square analysis was used to compare the proportion of intestinal tumors in $Tgfbr1^{+/-}$ and $Tgfbr1^{+/+}$ mice and the proportion of colonic tumors in $Apc^{Min/+}$; $Tgfbr1^{+/-}$ and $Apc^{Min/+}$; $Tgfbr1^{+/+}$ mice.

Results

Generation of a novel mouse model of targeted Tgfbr1 inactivation

A knockout mouse model of *Tgfbr1* generated by targeted deletion of exon 3 has been previously described (23). There is growing evidence that the signal sequence of human TGFBR1*6A may have intrinsic biological effects, which are caused by mutations within the exon 1 GCG repeat sequence (21;22). While the exon 3 *Tgfbr1* knockout model does not result in the generation of functional Tgfbr1 (23), the generation of a functionally active signal sequence cannot be excluded. To circumvent this potential problem, we designed a classical knockout vector to insert a Neomycin resistance cassette (Neo) into a Not I site located immediately after the start codon and removing 1.1kb of mouse genomic sequence immediately upstream of this Not I site (Figure 1A). This approach precludes the generation of any signal sequence, which is encoded by part of the removed sequence. The $Tgfbr1^{+/-}$ mice were viable and fertile, and appeared normal in their morphology and behavior. A total of 50 pups from the heterozygous intercrosses were genotyped, and no $Tgfbr1^{-/-}$ pups were found, with only

the wild-types and the heterozygotes at the ratio of 1:2. Dead *Tgfbr1*$^{-/-}$ embryos were found at a ratio of 1:4 at the time of collection of MEFs. These findings are consistent with the previous report of targeted disruption of *Tgfbr1* exon 3 in which mice lacking *Tgfbr1* die at midgestation (23). We did not therefore attempt to determine the stage of lethality. At 16-months, follow-up of 10 *Tgfbr1*$^{+/-}$ mice does not suggest increased mortality as compared with 10 wild-type littermates.

Tgfbr1 expression levels in different tissues were first compared by real-time PCR. Tgfbr1 expression in *Tgfbr1*$^{+/-}$ tissues ranged from 54% in embryonic fibroblasts to 62% in colonic epithelium, 44% in tail and 67% in blood lymphocytes when compared with corresponding expression levels in *Tgfbr1*$^{+/+}$ mice (Figure 1C). Tissue-specific differences between *Tgfbr1*$^{+/-}$ and *Tgfbr1*$^{+/+}$ mice were significant for each corresponding tissue, $p = 0.016$ for embryonic fibroblasts, $p = 0.04$ for colonic epithelium, $p = 0.009$ for tail, and $p=0.01$ for blood lymphocytes. The differences in Tgfbr1 expression levels between the various *Tgfbr1*$^{+/-}$ tissues were not statistically significant, $p = 0.429$. To assess the functional consequences of *Tgfbr1* haploinsufficiency we measured Tgfbr1 and Tgfbr2 protein expression in MEFs. Tgfbr1 expression levels were lower in the *Tgfbr1*$^{+/-}$ MEFs than in *Tgfbr1*$^{+/+}$ MEFs (Fig. 1D). As expected, Tgfbr2 levels were comparable (Figure 1D).

Tgfbr1 haploinsufficiency enhances tumor formation

Because the gastrointestinal tract is a common site of cancer in humans with constitutively altered TGF-β signaling (1;16), we tested the effect of *Tgfbr1* haploinsufficiency on *Apc*$^{Min/+}$ -mediated intestinal tumorigenesis. *Apc*$^{Min/+}$ mice harbor a premature stop codon in one allele of the *Apc* tumor suppressor gene (*Apc*$^{Min/+}$). These mice develop multiple intestinal adenomas and mimic human familial adenomatosis polyposis coli (24;25). *Tgfbr1*$^{+/-}$ female mice on the 129/SvIm background were backcrossed into the C57BL/6 background. F2 *Tgfbr1*$^{+/-}$ females were crossed with *Apc*$^{Min/+}$ male mice (C57BL/6). Mice were sacrificed at 12 weeks and examined for intestinal tumors. The tumors counted were verified by histology. We did not observe any tumors in the small and large bowels of 8 *Tgfbr1*$^{+/+}$ and 9 *Tgfbr1*$^{+/-}$ mice in wild type *Apc* background. A total of 9 *Apc*$^{Min/+}$; *Tgfbr1*$^{+/+}$ mice developed an average of 5.4 ± 1.7 tumors (mean ± S.E.M.) while the number of tumors observed in 10 *Apc*$^{Min/+}$; *Tgfbr1*$^{+/-}$ mice was almost three times higher: 14.5 ± 1.1 tumors (Figure 2A). The difference in the number of tumors between the two groups was highly significant: 9.8 tumors (95% CI, 4.8–13.4), $p = 0.0004$. The majority of tumors was small (less than 3 mm) and predominantly scattered in the small intestine. Five *Apc*$^{Min/+}$; *Tgfbr1*$^{+/-}$ mice (50%) had an average of 2.4 ± 0.2 colonic tumors while only two *Apc*$^{Min/+}$; *Tgfbr1*$^{+/+}$ mice (22%) had one colonic tumor each, a non-significant difference, $p = 0.437$. The identity of each lesion as tumor rather than lymphoid aggregates was confirmed in seven mice from each group by histopathology.

To determine the reproducibility of our initial findings obtained in a mixed 129SvIm × C57BL/6 background in 2006, we repeated these experiments with *Tgfbr1*$^{+/-}$ mice, which were fully backcrossed into the C57BL/6 using speed congenics markers (Supplemental Material). As seen in figure 2B, there was an average of 30.2 ± 0.9 tumors in 12 *Apc*$^{Min/+}$; *Tgfbr1*$^{+/+}$ mice and 61.4 ± 3.4 tumors in 7 *Apc*$^{Min/+}$; *Tgfbr1*$^{+/-}$ mice (mean ± S.E.M.). The difference in the number of tumors between the two groups was highly significant: 31.2 tumors (95% CI, 25.3–37.2), $p = 4.8 \times 10^{-5}$. Importantly, the number of colonic tumors was higher among *Apc*$^{Min/+}$; *Tgfbr1*$^{+/-}$ mice (4.9 ± 0.3) than among *Apc*$^{Min/+}$; *Tgfbr1*$^{+/+}$ mice (3.0 ± 0.4), $p = 0.0005$.

Six *Apc*$^{Min/+}$; *Tgfbr1*$^{+/-}$ mice (three in the mixed background and three in the pure C57BL/6 background) exhibited large colonic tumors with a maximal diameter greater than 7 mm (Figure 2C). Histological analysis of these polypoid and ulcerated colonic tumors revealed the presence of carcinoma (Figure 2D and 2E) as evidenced by the presence of distinct cytological and

nuclear atypia. The largest tumors in the $Apc^{Min/+}$; $Tgfbr1^{+/+}$ mice in either the mixed 129SvIm/C57BL/6 or the pure C57BL/6 backgrounds were 3 mm in size and none of them harbored carcinoma. Among all mice examined at 12 weeks the proportion of $Apc^{Min/+}$; $Tgfbr1^{+/-}$ mice with colonic tumors greater than 7 mm (35.3%) harboring carcinoma was significantly higher than that of $Apc^{Min/+}$; $Tgfbr1^{+/+}$ mice (0%), p = 0.018.

Tgfbr1 haploinsufficiency modifies TGF-β-mediated signaling and cell proliferation but does not alter hematopoiesis

Next we studied the effects of *Tgfbr1* haploinsufficiency on cell proliferation using mouse embryonic fibroblasts (MEFs) from $Tgfbr1^{+/+}$ and $Tgfbr1^{+/-}$ mice. In the absence of TGF-β, the growth of $Tgfbr1^{+/+}$ and $Tgfbr1^{+/-}$ MEFs was identical (Figure 3A). In the presence of exogenously added TGF-β, the proliferation of $Tgfbr1^{+/-}$ MEFs decreased by 38.32 ± 3.44% while that of $Tgfbr1^{+/+}$ MEFs decreased by 58.24 ± 5.74% (Figure 3B), p = 0.0005. To directly analyze the signaling activity of $Tgfbr1^{+/+}$ and $Tgfbr1^{+/-}$ MEFs, we used as readouts the TGF-β reporter 3TP-lux (26) and the TGF-β reporter SBE4-Lux (27). As seen in Figure 3C, following addition of TGF-β to the cell culture medium, induction of TGF-β signaling was significantly higher for $Tgfbr1^{+/+}$ than $Tgfbr1^{+/-}$ MEFs for 3TP-Lux (3.62 fold vs 2.73 fold) (p = 0.02) and SBE4-Lux (5.76 fold vs 4.47 fold) (p = 0.04). The differences between $Tgfbr1^{+/+}$ and $Tgfbr1^{+/-}$ with respect to the induction of SBE4-Lux and 3TP-Lux upon exposure to TGF-β were almost similar, 24.6% and 22.4%, respectively.

Because the TGF-β signaling pathway is a potent regulator of hematopoietic differentiation (28) and because alterations in lymphocyte TGF-β signaling have been implicated in colorectal tumor progression in mice (8;29), we sought to determine whether *Tgfbr1* haploinsufficiency had any measurable effects on the hematopoietic compartment. Complete blood counts of five $Tgfbr1^{+/-}$ and five $Tgfbr1^{+/+}$ mice obtained at 12 weeks did not reveal any difference in the average red blood cell, white blood cell or platelet numbers, thus indicating that *Tgfbr1* haploinsufficiency alone does not significantly alter hematopoiesis. The average lymphocyte count was 13.11 ± 0.31 and 12.73 ± 0.55 (mean ± S.D.) for $Tgfbr1^{+/-}$ and $Tgfbr1^{+/+}$ mice, respectively, a non-significant difference, p = 0.181.

Tgfbr1 haploinsufficiency impairs Smad2 and Smad3 signaling

We first assessed the levels of TGF-β-mediated generation of pSmad2 in $Tgfbr1^{+/+}$ and $Tgfbr1^{+/-}$ MEFs over 24 hours. While pSmad2 levels were almost identical at 1 and 4 hr, pSmad2 levels decreased by approximately 50% at 8 hr and 80% at 24 hr in $Tgfbr1^{+/-}$ MEFs while they decreased only slightly in $Tgfbr1^{+/+}$ MEFs (Figure 4A). It has been previously shown that phosphorylation of Smad3 is an essential step in signal transduction by TGF-β for inhibition of cell proliferation (30) and *Smad3*-deficient mice are prone to colon cancer development (7;31). To assess the impact of *Tgfbr1* haploinsufficiency on the phosphorylation of Smad3 we use an antibody targeting the $Ser^{423/425}$ site on Smad3 (32;33). As seen in Figure 4B, following exposure to TGF-β pSmad3 levels were higher at 1 and 16 h in $Tgfbr1^{+/+}$ MEFs than in $Tgfbr1^{+/-}$ MEFs. Hence, *Tgfbr1* haploinsufficiency was associated with a small but significant decrease in TGF-β signaling mediated by decreased phosphorylation of both Smad2 and Smad3.

Downstream effects of decreased Tgfbr1-mediated signaling in vitro

To dissect the downstream effects of decreased TGF-β signaling we assessed the expression levels of selected mediators of the cell cycle and downstream effectors of TGF-β signaling. As seen on Figure 4C, there was no difference in the levels of these mediators in the absence of TGF-β with the exception of mildly decreased baseline levels of Ccnd1 in $Tgfbr1^{+/+}$ MEFs when compared with $Tgfbr1^{+/-}$ MEFs. This differential expression pattern was markedly enhanced following exposure to TGF-β as exemplified by reduced Ccnd1 expression in

Tgfbr1$^{+/+}$ MEFs after 4 hours while Ccnd1 levels initially increased and remained elevated at 16 hours in *Tgfbr1*$^{+/-}$ MEFs (Figure 4C). Levels of Cdkn2b remained unchanged upon exposure to TGF-β in *Tgfbr1*$^{+/+}$ MEFs while we observed a small decrease in Cdkn2b levels in *Tgfbr1*$^{+/-}$ MEFs. The emergence of differential expression of pSmad2 (Figure 4A), pSmad3 (Figure 4B) and Ccnd1 (Figure 4C) levels occurred in parallel, which suggests that decreased Smad signaling results in persistently high Ccnd1 levels in *Tgfbr1*$^{+/-}$ MEFs.

Characterization of Tgfbr1 haploinsufficiency effects on the intestinal epithelium

To characterize the *in vivo* consequences of constitutively decreased TGF-β signaling, we performed pSmad2 immunostaining of normal appearing intestinal tissue and tumor sections. While pSmad2 staining was homogeneous throughout the intestinal mucosa of *Apc*$^{Min/+}$; *Tgfbr1*$^{+/+}$ mice (Figure 5A), we observed reduced pSmad2 staining in the crypts but not in the villi of *Apc*$^{Min/+}$; *Tgfbr1*$^{+/-}$ mice (Figure 5B). To comprehensively assess the impact of *Tgfbr1* haploinsufficiency on Smad-mediated TGF-β signaling we also performed pSmad3 immunostaining of the same tissues. As seen in Figure 5C, we observed homogeneous pSmad3 staining in the crypts of *Apc*$^{Min/+}$; *Tgfbr1*$^{+/+}$ mice while pSmad3 staining was markedly reduced in the crypts of *Apc*$^{Min/+}$; *Tgfbr1*$^{+/-}$ mice (Figure 5D), mirroring the pSmad2 findings and demonstrating that *Tgfbr1* haploinsufficiency results in decreased phosphorylation of both receptor Smads within the intestinal epithelial crypts thus resulting in overall decreased Smad-mediated TGF-β signaling *in vivo.* To determine whether the differential expression of Smads within the intestinal crypts modifies cellular proliferation *in vivo*, we assessed the levels of proliferating cell nuclear antigen (PCNA) in the normal intestinal epithelium of *Apc*$^{Min/+}$; *Tgfbr1*$^{+/+}$ and *Apc*$^{Min/+}$; *Tgfbr1*$^{+/-}$ mice. PCNA staining was significantly more intense in *Apc*$^{Min/+}$; *Tgfbr1*$^{+/-}$ mice (62.2 ± 2.2% positive staining) (Figure 5F) than in their wild type counterpart (44.4 ± 2.8% positive staining) (Figure 5E) ($p = 0.008$), thus confirming *in vivo* the observed *in vitro* increased cellular proliferation of *Tgfbr1*$^{+/-}$ upon exposure to TGF-β.

Characterization of Tgfbr1 haploinsufficiency effects on intestinal tumors

Tumors arising from both *Apc*$^{Min/+}$; *Tgfbr1*$^{+/+}$ and *Apc*$^{Min/+}$; *Tgfbr1*$^{+/-}$ mice had uniform pSmad staining reflecting preserved *in vivo* Smad signaling. However, we found focal areas of decreased pSmad2 staining among *Apc*$^{Min/+}$; *Tgfbr1*$^{+/-}$ mice tumors (Fig. 6B) but not in their wild type counterparts (Fig. 6A). Consistent with the findings of preserved TGF-β signaling activity in the tumors of both *Apc*$^{Min/+}$; *Tgfbr1*$^{+/+}$ and *Apc*$^{Min/+}$; *Tgfbr1*$^{+/-}$ mice, we found no evidence of *Tgfbr1* loss of heterozygosity in six microdissected colonic tumors from three different *Apc*$^{Min/+}$; *Tgfbr1*$^{+/-}$ mice (Supplemental Table 2). The combined evidence from pSmad2 IHC as well as LOH analysis of intestinal tumors demonstrate that reduced dosage rather than abrogation of Tgfbr1-mediated Smad signaling is sufficient to enhance the *Apc*-mediated development of intestinal tumors and adenocarcinoma at 12 weeks.

The role of Ccnd1 as a mediator of colon cancer development and progression is reflected by the fact that decreased Ccnd1 expression reduces tumor formation in *Apc*$^{Min/+}$ mice (34). Conversely, the role of the Wnt pathway in promoting intestinal stem cell proliferation has been previously documented (35). Located in the intestinal crypts, stem cells constantly generate progeny that differentiate as they flow upward to the tip of the villi, where they die within days. TCF-mediated induction of c-Myc, with secondary induction of Ccnd1, is thought to drive proliferation in these cells and their malignant derivatives (35). To assess the downstream effects of decreased Tgfbr1-mediated TGF-β signaling on Ccnd1 *in vivo* we measured the levels of Ccnd1 by IHC and found that Ccnd1 staining was significantly higher in the tumors of *Apc*$^{Min/+}$; *Tgfbr1*$^{+/-}$ mice (50.7 ± 4.1% positive staining) (Figure 6D) than in those of *Apc*$^{Min/+}$; *Tgfbr1*$^{+/+}$ mice (20.1 ± 5.7% positive staining) (Figure 6C) ($p = 0.002$).

To determine whether *Tgfbr1* haploinsufficiency modifies tumor proliferation *in vivo*, we assessed the levels of proliferating cell nuclear antigen (PCNA) in tumors of $Apc^{Min/+}$; $Tgfbr1^{+/+}$ and $Apc^{Min/+}$; $Tgfbr1^{+/-}$ mice. PCNA staining was significantly more intense in $Apc^{Min/+}$; $Tgfbr1^{+/-}$ tumors (82.0 ± 2.9% positive staining) (Figure 6F) than in their wild type counterpart (48.2 ± 3.8% positive staining) (Figure 6E) ($p = 0.0003$), thus establishing *in vivo* that decreased but not abrogated Tgfbr1-mediated signaling confers a selective growth advantage to tumor cells.

Discussion

The significant difference in the number of intestinal tumors observed in both mixed 129SvIm × C57BL/6 and pure C57BL/6 backgrounds provides strong support for the novel concept that decreased Tgfbr1-mediated signaling results in the enhanced cell proliferation of normal appearing intestinal epithelial cells within the crypts as well as tumor cells in the presence of preserved TGF-β signaling. Similarly to what was originally observed with the *cis-*$Apc^{+/\Delta 716}$ $Smad4^{+/-}$ mice in which TGF-β signaling is completely abrogated (5), we found essentially the same results with the F3 (C57BL/6) backcross generation and the fully backcrossed (C57BL/6) generation, except for higher intestinal polyp numbers. It has been previously hypothesized that the reduced polyp numbers in mice with a mixed 129SvIm × C57BL6 background is presumably due by the background gene(s) brought in from the 129SvIm strain (5). Immunohistochemistry analysis show that PCNA levels were inversely correlated with pSmad2 and pSmad3 levels in the intestinal crypts, providing strong support for the notion that increased cellular proliferation is a direct consequence of decreased pSmad2/pSmad3-mediated signaling.

Existing mouse intestinal tumor models based on somatic *Apc* inactivation display mainly small intestinal lesions, and carcinomas are rare (36;37). Inactivation of one copy of the *Smad4* gene accelerated tumor progression from intestinal polyps to adenocarcinoma in compound heterozygous *cis-*$Apc^{+/\Delta 716}$ $Smad4^{+/-}$ mice while control *cis-*$Apc^{+/\Delta 716}$ mice developed adenomas but not adenocarcinomas (5). However, tumor epithelial cells in *cis-*$Apc^{+/\Delta 716}$ $Smad4^{+/-}$ mice carry homozygous mutations in both *Apc* and *Smad4*, and there is no evidence of Smad4 protein expression in the colorectal tumor cells (38). This results in complete abrogation of Smad-mediated TGF-β signaling within intestinal tumors. Similar results have been reported in mice in which the *Tgfbr2* allele was knocked out in the intestinal epithelium (6). In both models, complete abrogation of TGF-β signaling was required to induce malignant transformation of intestinal neoplasms initiated by *Apc* mutation. Our findings constitute the first report of decreased but not abrogated TGF-β signaling resulting in adenocarcinoma formation at 3 months. It is also the first report of constitutively altered but not abrogated TGF-β signaling upstream of Smad4 associated with increased colorectal tumor development. These results provide strong evidence that constitutively altered Tgfbr1-mediated TGF-β signaling is a potent modified of colorectal carcinogenesis. Our initial results with mice bred in a mixed background prompted us to investigate the relevance of this novel concept in human colorectal carcinogenesis. This led to the discovery that germline decreased expression of TGFBR1 is a quantitative trait that occurs in 10–20% of patients with MSI-negative colorectal cancer and in 1–3% of healthy controls (18). This trait is dominantly inherited, segregates in families and confers a substantially increased risk of colorectal cancer (18).

Decreased Tgfbr1 signaling leads to decreased levels of phosphorylated Smad2 and Smad3 in MEFs, in *in vitro* experiments, and *in vivo* in the normal appearing colonic epithelium, thus resulting in a global decrease of Smad-mediated signaling. This was observed *in vitro* upon addition of exogenous TGF-β but was only observed in the intestinal crypts and in patches within tumors *in vivo*. Interestingly, the same pattern of decreased SMAD-signaling was observed in the lymphocytes of patients with colorectal cancer and evidence of constitutively

decreased expression of TGFBR1 (18). This highlights the critical role of Tgfbr1 as a potentially limiting factor with respect to the activation of the Smad-signaling cascade at sites of either high TGF-β secretion and/or high cellular proliferation. The absence of effective downregulation of Ccnd1 in *Tgfbr1*$^{+/-}$ MEFs and the observed increased Ccnd1 levels within the tumors of *Apc*$^{Min/+}$; *Tgfbr1*$^{+/-}$ mice provide the first evidence of the downstream effects of decreased Smad-mediated TGF-β signaling. The TGF-β responses in epithelial cells involve the induction of Cdkn2b by means of the Smads (39). Increased Cdkn2b levels are an important aspect of the TGF-β cytostatic program leading to decreased Ccnd1 expression (40). The decreased Cdkn2b levels observed in *Tgfbr1*$^{+/-}$ MEFs provide a plausible link between decreased Smad-mediated signaling and increased Ccnd1 expression. The absence of any obvious phenotype in *Tgfbr1*$^{+/-}$ mice as well as the absence of phenotypic traits in human beings with constitutionally-reduced *TGFBR1* expression (18) suggests that decreased Tgfbr1-mediated TGF-β signaling does not affect normal development. One potential explanation is that decreased Tgfbr1 signaling only becomes a limiting factor when persistently decreased phosphorylation of Smad2 and Smad3 leads to decreased TGF-β signaling, which in turn results in higher cell proliferation. As mutations of the *APC* gene are among the most commonly encountered genetic hallmarks of human colorectal cancer (4;41), altered Tgfbr1 signaling is emerging as a potent modifier of colorectal cancer development. The impact of decreased Tgfbr1-mediated signaling leading to decreased Smad2 and Smad3 signaling is further highlighted by the recent discovery that both *SMAD2* and *SMAD3* are among the most commonly mutated genes in human colorectal cancer (4) acting as crucial mediators of colon carcinogenesis.

Thorough histological review of the normal appearing colorectal epithelium and tumor tissues did not reveal difference in the numbers of inflammatory cells in either mouse strain. Together with the findings of comparable lymphocyte counts in *Apc*$^{Min/+}$; *Tgfbr1*$^{+/-}$ and *Apc*$^{Min/+}$; *Tgfbr1*$^{+/+}$ mice at 12 weeks, this argues against a major role of inflammation as a contributor to the tumor phenotype observed in *Apc*$^{Min/+}$; *Tgfbr1*$^{+/-}$ mice. Nonetheless, TGF-β in tumor infiltrating lymphocytes has been shown to control the growth of dysplastic epithelial cells in experimental colon cancer (29). Furthermore, abrogation of TGF-β signaling within T-cells by means of *Smad4* inactivation leads to gastrointestinal cancer development (8). These findings suggest that alterations in lymphocyte-mediated TGF-β signaling may contribute to colorectal cancer development in *Apc*$^{Min/+}$; *Tgfbr1*$^{+/-}$ mice through a “landscaping” effect (42). Additional studies will be needed to clarify the role of decreased Tgfbr1-mediated signaling and assess potential qualitative differences between *Tgfbr1*$^{+/-}$ and *Tgfbr1*$^{+/-}$ lymphocytes and stromal cells.

In summary, our data provide a strong rationale and a plausible mechanism for the novel concept that *Tgfbr1* haploinsufficiency has a causative role in intestinal carcinogenesis. *Apc*$^{Min/+}$; *Tgfbr1*$^{+/-}$ mice may therefore emerge as a valuable human-based mouse model for studying colorectal cancer development and progression.

Supplementary Material

Refer to Web version on PubMed Central for supplementary material.

Acknowledgments

Supported by grants from the Walter S. Mander Foundation, Chicago, IL, the Jeannik M. Littlefield-AACR Grant in Metastatic Colon Cancer Research, and grants CA112520, CA108741, CA67941 and CA16058 from the NCI.

Reference List

1. Howe JR, Sayed MG, Ahmed AF, Ringold J, Larsen-Haidle J, Merg A, et al. The prevalence of MADH4 and BMPR1A mutations in juvenile polyposis and absence of BMPR2, BMPR1B, and ACVR1 mutations. J Med Genet 2004 Jul;41(7):484–491. [PubMed: 15235019]
2. Broderick P, Carvajal-Carmona L, Pittman AM, Webb E, Howarth K, Rowan A, et al. A genome-wide association study shows that common alleles of SMAD7 influence colorectal cancer risk. Nat Genet 2007 Nov;39(11):1315–1317. [PubMed: 17934461]
3. Xie W, Rimm DL, Lin Y, Shih WJ, Reiss M. Loss of Smad signaling in human colorectal cancer is associated with advanced disease and poor prognosis. Cancer J 2003 Jul;9(4):302–312. [PubMed: 12967141]
4. Sjoblom T, Jones S, Wood LD, Parsons DW, Lin J, Barber TD, et al. The Consensus Coding Sequences of Human Breast and Colorectal Cancers. Science 2006 Oct 13;314(5797):268–274. [PubMed: 16959974]
5. Takaku K, Oshima M, Miyoshi H, Matsui M, Seldin MF, Taketo MM. Intestinal tumorigenesis in compound mutant mice of both dpc4 (Smad4) And apc genes. Cell 1998 Mar 6;92(5):645–656. [PubMed: 9506519]
6. Munoz NM, Upton M, Rojas A, Washington MK, Lin L, Chytil A, et al. Transforming Growth Factor {beta} Receptor Type II Inactivation Induces the Malignant Transformation of Intestinal Neoplasms Initiated by Apc Mutation. Cancer Res 2006 Oct 15;66(20):9837–9844. [PubMed: 17047044]
7. Sodir NM, Chen X, Park R, Nickel AE, Conti PS, Moats R, et al. Smad3 Deficiency Promotes Tumorigenesis in the Distal Colon of ApcMin/+ Mice. Cancer Res 2006 Sep 1;66(17):8430–8438. [PubMed: 16951153]
8. Kim BG, Li C, Qiao W, Mamura M, Kasperczak B, Anver M, et al. Smad4 signalling in T cells is required for suppression of gastrointestinal cancer. Nature 2006 Jun 22;441(7096):1015–1019. [PubMed: 16791201]
9. Hohenstein P, Molenaar L, Elsinga J, Morreau H, van der KH, Struijk A, et al. Serrated adenomas and mixed polyposis caused by a splice acceptor deletion in the mouse Smad4 gene. Genes Chromosomes Cancer 2003 Mar;36(3):273–282. [PubMed: 12557227]
10. Taketo MM, Takaku K. Gastro-intestinal tumorigenesis in Smad4 mutant mice. Cytokine & Growth Factor Reviews 2000 Mar;11(1–2):147–157. [PubMed: 10708962][Review] [41 refs].
11. Alberici P, Jagmohan-Changur S, de PE, van dV, Smits R, Hohenstein P, et al. Smad4 haploinsufficiency in mouse models for intestinal cancer. Oncog 2006 Mar 23;25(13):1841–1851.
12. Pasche B, Luo Y, Rao PH, Nimer SD, Dmitrovsky E, Caron P, et al. Type I transforming growth factor beta receptor maps to 9q22 and exhibits a polymorphism and a rare variant within a polyalanine tract. Cancer Res 1998 Jul 1;58(13):2727–2732. [PubMed: 9661882]
13. Chen T, de Vries EG, Hollema H, Yegen HA, Vellucci VF, Strickler HD, et al. Structural alterations of transforming growth factor-beta receptor genes in human cervical carcinoma. Int J Cancer 1999 Jul 2;82(1):43–51. [PubMed: 10360819]
14. Pasche B, Kolachana P, Nafa K, Satagopan J, Chen YG, Lo RS, et al. T beta R-I(6A) is a candidate tumor susceptibility allele. Cancer Res 1999 Nov 15;59(22):5678–5682. [PubMed: 10582683]
15. Bian Y, Caldes T, Wijnen J, Franken P, Vasen H, Kaklamani V, et al. TGFBR1*6A May Contribute to Hereditary Colorectal Cancer. J Clin Oncol 2005 May 1;23(13):3074–3078. [PubMed: 15860866]
16. Xu Y, Pasche B. TGF-{beta} signaling alterations and susceptibility to colorectal cancer. Hum Mol Genet 2007 Apr 15;16 Spec No 1:R14–R20. [PubMed: 17613544]
17. Kaklamani VG, Baddi L, Liu J, Rosman D, Phukan S, Bradley C, et al. Combined Genetic Assessment of Transforming Growth Factor-{beta} Signaling Pathway Variants May Predict Breast Cancer Risk. Cancer Res 2005 Apr 15;65(8):3454–3461. [PubMed: 15833881]
18. Valle L, Serena-Acedo T, Liyanarachchi S, Hampel H, Comeras I, Li Z, et al. Germline Allele-specific Expression of TGFBR1 Confers an Increased Risk of Colorectal Cancer. Science 2008 Aug 14;:1159397.
19. Hogan, B.; Beddington, R.; Costantini, F.; Lacy, E. Manipulating the mouse embryo. Vol. 2nd ed. Cold Spring Harbor Laboratory Press; 1994.

20. Tsutsui T, Hesabi B, Moons DS, Pandolfi PP, Hansel KS, Koff A, et al. Targeted disruption of CDK4 delays cell cycle entry with enhanced p27(Kip1) activity. Molecular & Cellular Biology 1999 Oct; 19(10):7011–7019. [PubMed: 10490638]
21. Pasche B, Knobloch TJ, Bian Y, Liu J, Phukan S, Rosman D, et al. Somatic Acquisition and Signaling of TGFBR1*6A in Cancer. JAMA: The Journal of the American Medical Association 2005 Oct 5;294 (13):1634–1646. [PubMed: 16204663]
22. Rosman DS, Phukan S, Huang CC, Pasche B. TGFBR1*6A Enhances the Migration and Invasion of MCF-7 Breast Cancer Cells through RhoA Activation. Cancer Res 2008 Mar 1;68(5):1319–1328. [PubMed: 18316594]
23. Larsson J, Goumans MJ, Sjostrand LJ, van Rooijen MA, Ward D, Leveen, et al. Abnormal angiogenesis but intact hematopoietic potential in TGF-beta type I receptor-deficient mice. EMBO Journal 2001 Apr 2;20(7):1663–1673. [PubMed: 11285230]
24. Moser AR, Pitot HC, Dove WF. A dominant mutation that predisposes to multiple intestinal neoplasia in the mouse. Science 1990 Jan 19;247(4940):322–324. [PubMed: 2296722]
25. Su LK, Kinzler KW, Vogelstein B, Preisinger AC, Moser AR, Luongo C, et al. Multiple intestinal neoplasia caused by a mutation in the murine homolog of the APC gene. Science 1992 May 1;256 (5057):668–670. [PubMed: 1350108]
26. Carcamo J, Zentella A, Massague J. Disruption of transforming growth factor beta signaling by a mutation that prevents transphosphorylation within the receptor complex. Mol Cell Biol 1995;15:1573–1581. [PubMed: 7862150]
27. Zawel L, Dai JL, Buckhaults P, Zhou S, Kinzler KW, Vogelstein B, et al. Human Smad3 and Smad4 are sequence-specific transcription activators. Mol Cell 1998 Mar;1(4):611–617. [PubMed: 9660945]
28. Dong M, Blobe GC. Role of transforming growth factor-beta in hematologic malignancies. Blood 2006 Jun 15;107(12):4589–4596. [PubMed: 16484590]
29. Becker C, Fantini MC, Schramm C, Lehr HA, Wirtz S, Nikolaev A, et al. TGF-beta suppresses tumor progression in colon cancer by inhibition of IL-6 trans-signaling. Immunity 2004 Oct;21(4):491–501. [PubMed: 15485627]
30. Liu XD, Sun Y, Constantinescu SN, Karam E, Weinberg RA, Lodish HF. Transforming growth factor beta-induced phosphorylation of smad3 is required for growth inhibition and transcriptional induction in epithelial cells. Proc 1997 Sep 30;94(20):10669–10674.
31. Zhu YA, Richardson JA, Parada LF, Graff JM. Smad3 mutant mice develop metastatic colorectal cancer. Cell 1998 Sep 18;94(6):703–714. [PubMed: 9753318]
32. Yamagata H, Matsuzaki K, Mori S, Yoshida K, Tahashi Y, Furukawa F, et al. Acceleration of Smad2 and Smad3 Phosphorylation via c-Jun NH2-Terminal Kinase during Human Colorectal Carcinogenesis. Cancer Res 2005 Jan 1;65(1):157–165. [PubMed: 15665291]
33. Matsuzaki K. Smad3 phosphoisoform-mediated signaling during sporadic human colorectal carcinogenesis. Histol Histopathol 2006 Jun;21(6):645–662. [PubMed: 16528675]
34. Hulit J, Wang C, Li Z, Albanese C, Rao M, Di Vizio D, et al. Cyclin D1 Genetic Heterozygosity Regulates Colonic Epithelial Cell Differentiation and Tumor Number in ApcMin Mice. Molecular and Cellular Biology 2004 Sep 1;24(17):7598–7611. [PubMed: 15314168]
35. van de WM, Sancho E, Verweij C, de Lau W, Oving I, Hurlstone A, et al. The beta-catenin/TCF-4 complex imposes a crypt progenitor phenotype on colorectal cancer cells. Cell 2002 Oct 18;111(2): 241–250. [PubMed: 12408868]
36. Hinoi T, Akyol A, Theisen BK, Ferguson DO, Greenson JK, Williams BO, et al. Mouse Model of Colonic Adenoma-Carcinoma Progression Based on Somatic Apc Inactivation. Cancer Res 2007 Oct 15;67(20):9721–9730. [PubMed: 17942902]
37. Boivin(*) G, double d, Yang([sect]) K, Ward(‖) J, Pretlow([para]) T, Russell # , et al. Pathology of mouse models of intestinal cancer: Consensus report and recommendations. Gastroenterology 2003 Mar;124(3):762–777. [PubMed: 12612914]
38. Kitamura T, Kometani K, Hashida H, Matsunaga A, Miyoshi H, Hosogi H, et al. SMAD4-deficient intestinal tumors recruit CCR1+ myeloid cells that promote invasion. Nat Genet 2007 Apr;39(4): 467–475. [PubMed: 17369830]

39. Massague J. G1 cell-cycle control and cancer. Nature 2004 Nov 18;432(7015):298–306. [PubMed: 15549091]

40. Siegel PM, Massague J. Cytostatic and apoptotic actions of TGF-beta in homeostasis and cancer. Nat Rev Cancer 2003 Nov;3(11):807–820. [PubMed: 14557817]

41. Groden J, Thliveris A, Samowitz W, Carlson M, Gelbert L, Albertsen H, et al. Identification and characterization of the familial adenomatous polyposis coli gene. Cell 1991 Aug 9;66(3):589–600. [PubMed: 1651174]

42. Kinzler KW, Vogelstein B. Landscaping the cancer terrain. Science 1998 May 15;280(5366):1036–1037. [PubMed: 9616081]

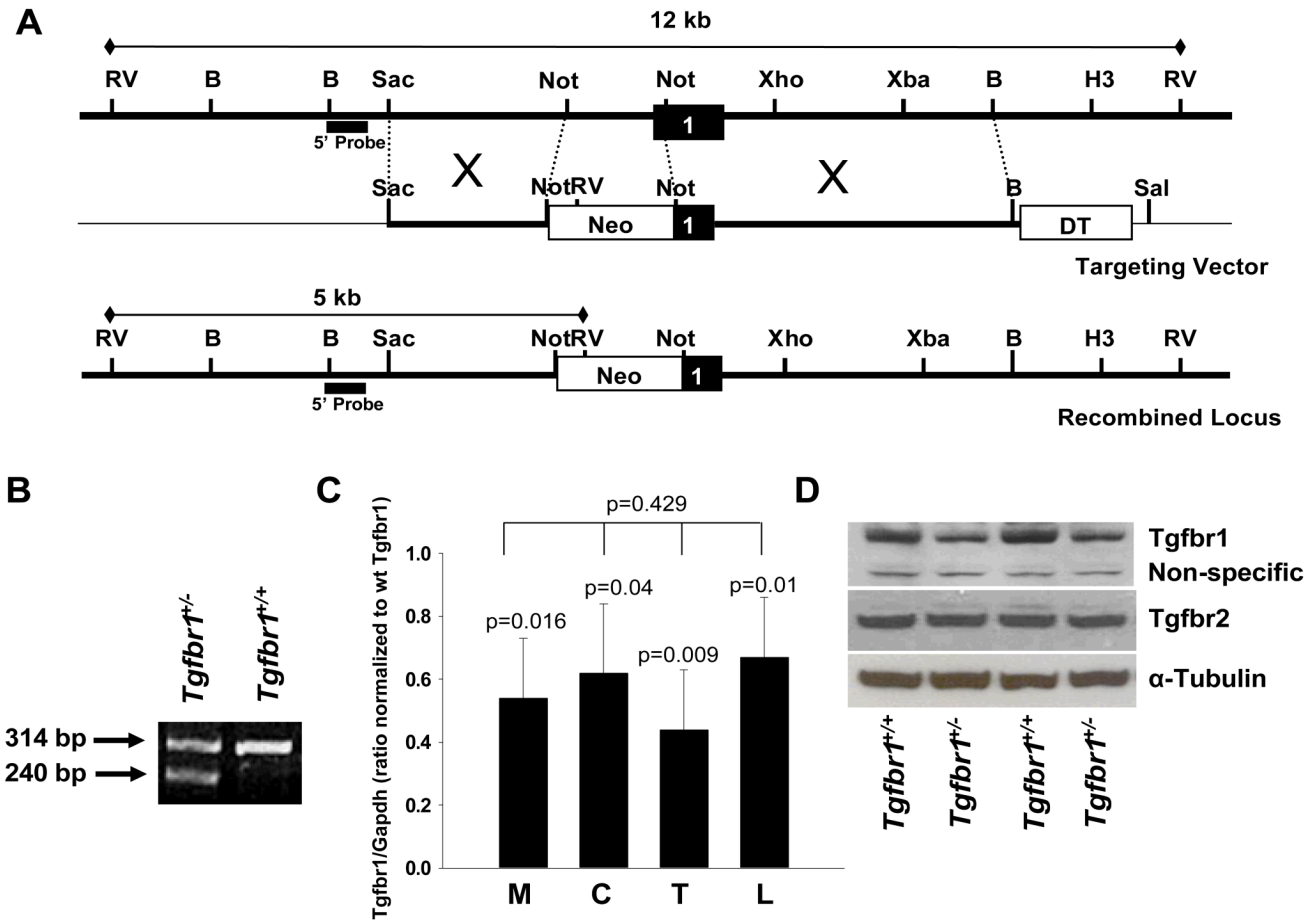

Figure 1. Generation of a novel *Tgfbr1* exon knockout mouse model

(A) Strategy for interrupting the *Tgfbr1* open reading frame by insertion of a Neo cassette. A classical targeting vector inserting was generated by inserting a Neomycin resistance cassette (Neo) into a Not I site located immediately after the start codon and removing 1.1kb of mouse genomic sequence immediately upstream of this Not I site.

(B) PCR genotyping for the $Tgfbr1^{+/-}$ allele using 3 primers reveals a 2nd band at 240 bp, corresponding to the knocked out allele, and the wildtype *Tgfbr1* band at 314 bp.

(C) Quantitative RT-PCR assessment of Tgfbr1 expression levels in mouse embryonic fibroblasts (M), colon intestinal tissue (C), tail (T), and peripheral lymphocytes (L) of $Tgfbr1^{+/+}$ and $Tgfbr1^{+/-}$ mice. Tissues were collected from three animals of each genotype. Each experiment was performed at least three times in triplicates. Tgfbr1 levels in $Tgfbr1^{+/-}$ tissues are expressed as ratio of Tgfbr1/Gapdh compared to each corresponding $Tgfbr1^{+/+}$ tissue.

(D) Western blot analysis of Tgfbr1 and Tgfbr2 expression of two representative pairs of MEFs from $Tgfbr1^{+/+}$ and $Tgfbr1^{+/-}$ mice.

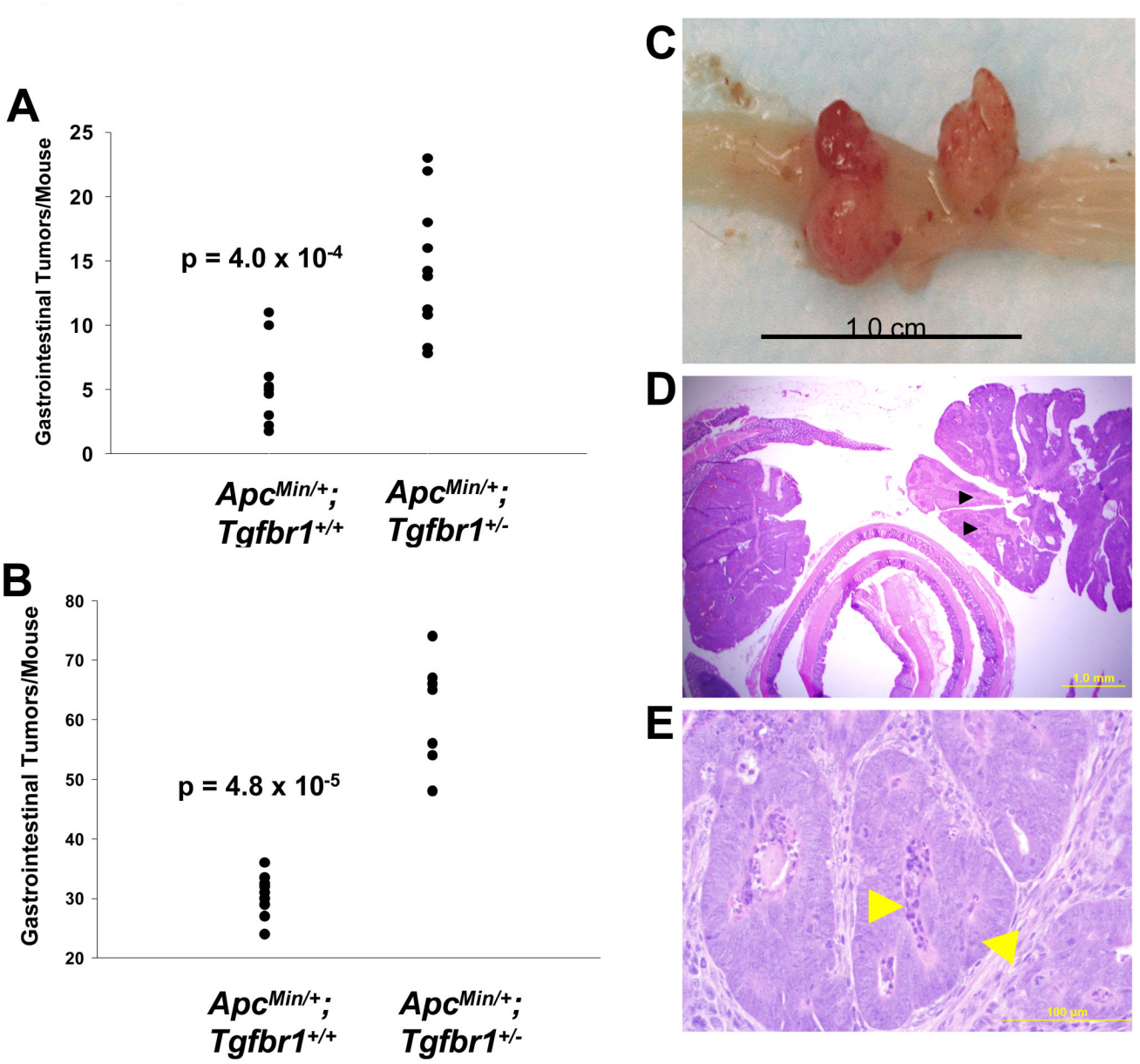

Figure 2. Tumorigenesis of *Apc*$^{Min/+}$;*Tgfbr1*$^{+/+}$ and *Apc*$^{Min/+}$;*Tgfbr1*$^{+/-}$ mice

(A and B) Number of gastrointestinal tumors per mouse at 12 weeks of age for *Apc*$^{Min/+}$;*Tgfbr1*$^{+/+}$ mice (n = 9) and *Apc*$^{Min/+}$;*Tgfbr1*$^{+/-}$ littermates (n = 10) in mixed 129Svlm/C57BL/6 background (A) and *Apc*$^{Min/+}$;*Tgfbr1*$^{+/+}$ mice (n = 12) and *Apc*$^{Min/+}$;*Tgfbr1*$^{+/-}$ littermates (n = 7) in C57BL/6 background (B). The data represents mean ± S.E.M.

(C) Large polyps arising from *Apc*$^{Min/+}$; *Tgfbr1*$^{+/-}$ mouse colonic mucosa at 12 weeks. Scale bar, 1cm.

(D–E) Histological analysis of the large polypoid colonic tumor from the *Apc*$^{Min/+}$; *Tgfbr1*$^{+/-}$ mouse shown in (C). (D) Black arrowheads represent presence of carcinoma. Scale bar, 1mm. (E) Enlarged view from part of the colonic polypoid tumor shown in D): Left arrow: central luminal necrosis, Right arrow: cribriform architecture with highly pleomorphic nuclei. Scale bar, 100 µM.

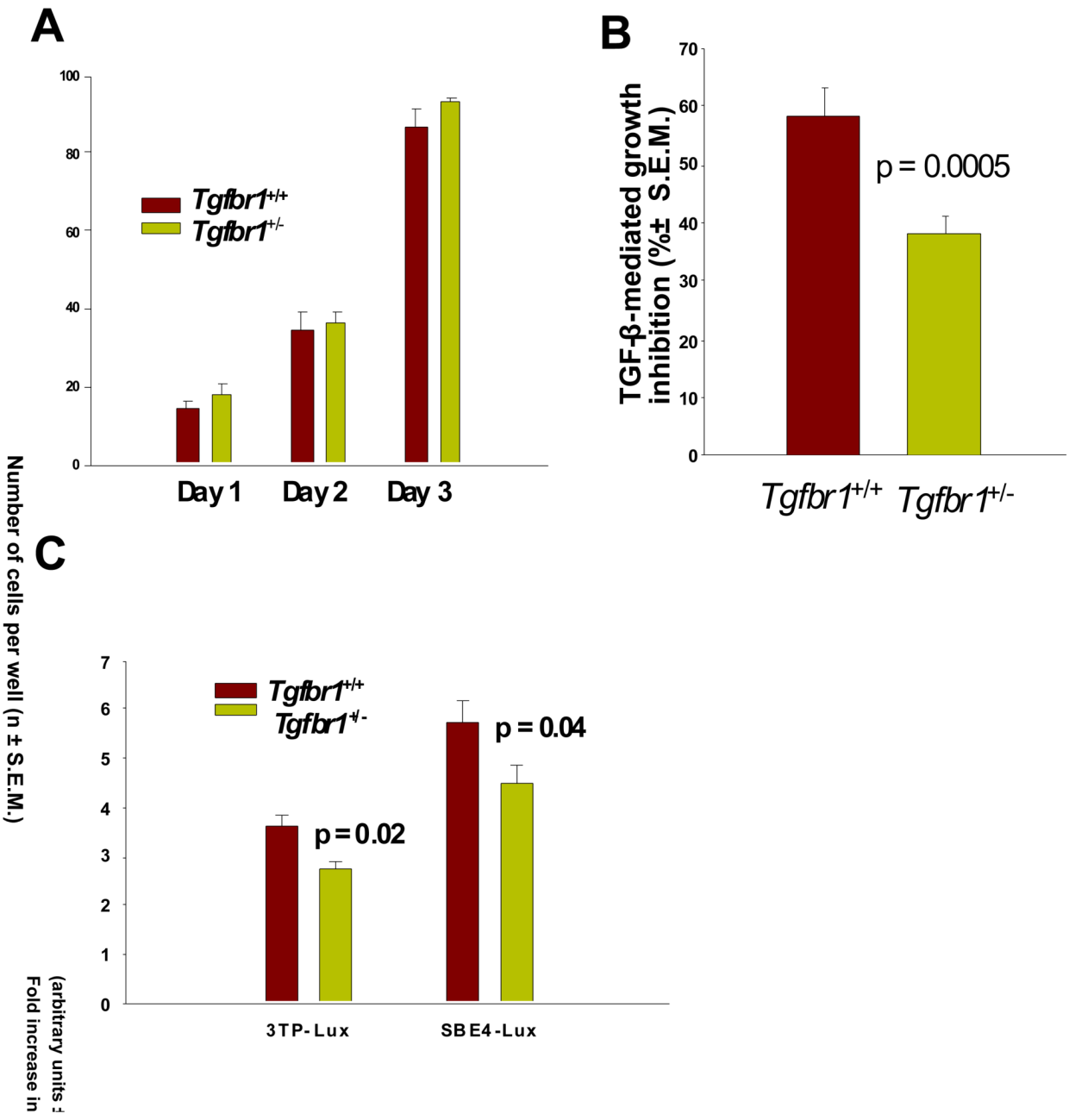

Figure 3. TGF-β-mediated cell proliferation of *Tgfbr1*$^{+/+}$ and *Tgfbr1*$^{+/-}$ mouse embryonic fibroblasts (MEFs)

(A) Spontaneous cell proliferation of *Tgfbr1*$^{+/+}$ and *Tgfbr1*$^{+/-}$ MEFs. Cell proliferation was assessed daily for three days by counting cells. The experiments were performed three times in triplicates. The data show mean cell count ± S.E.M.

(B) TGF-β-mediated cell proliferation assays. TGF-β-mediated cell proliferation was assessed in *Tgfbr1*$^{+/-}$ and *Tgfbr1*$^{+/+}$ MEFs exposed to 100 pM TGF-β1 for 24 hours. Cell proliferation was assessed by thymidine incorporation. The experiments were performed three times in triplicates. The data show mean TGF-β growth inhibition in % ± S.E.M.

(C) Direct measurement of TGF-β signaling using the 3TP-Lux and SBE4-Lux reporter assays in *Tgfbr1*$^{+/+}$ and *Tgfbr1*$^{+/-}$ MEFs following exposure to 100 pM TGF-β. Data represent the average of three experiments performed in triplicates. The data show fold increase in arbitrary units ± S.E.M.

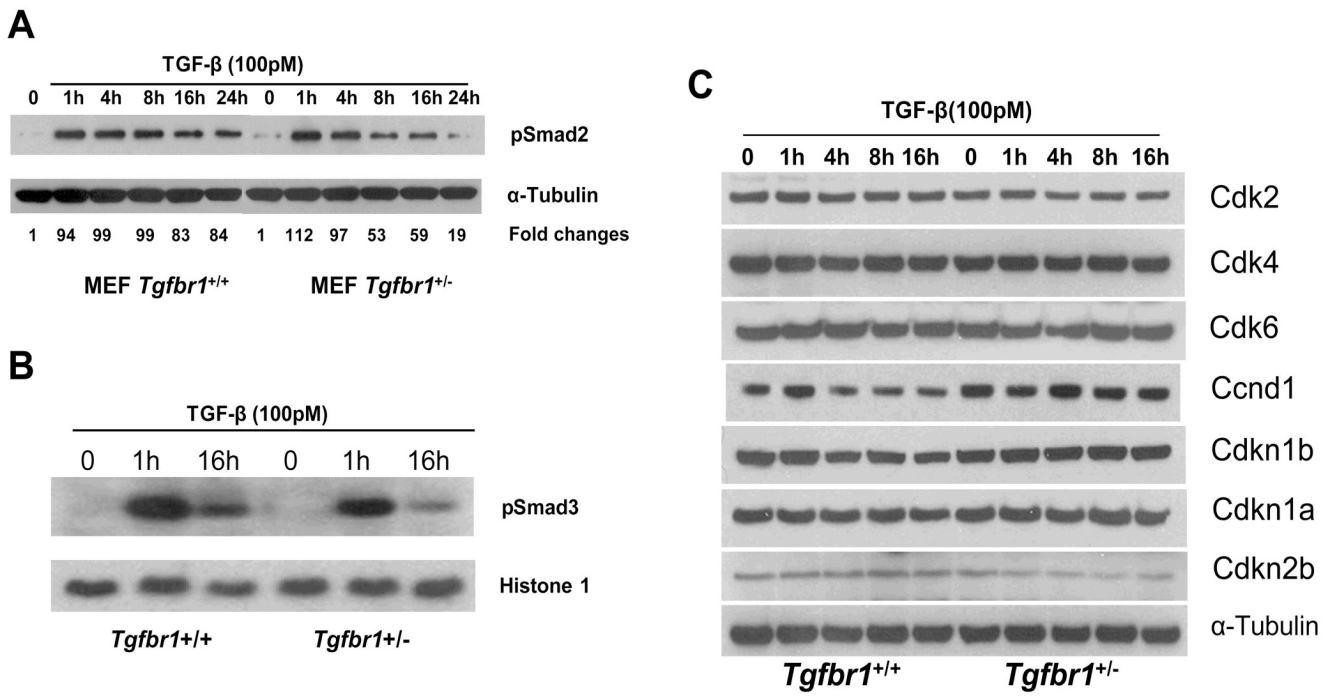

Figure 4. TGF-β-mediated Smad signaling of *Tgfbr1*$^{+/+}$ and *Tgfbr1*$^{+/-}$ mouse embryonic fibroblasts (MEFs)

(A) Assessment of pSmad2. Levels of phosphorylated Smad2 (pSmad2) following exposure of MEFs to TGF-β1 were assessed in three pairs of *Tgfbr1*$^{+/+}$ and *Tgfbr1*$^{+/-}$ MEFs from six different mice. The MEF pair presented is representative of the three pairs of MEFs.

(B) Assessment of pSmad3. Levels of phosphorylated Smad3 (pSmad3) following exposure of MEFs to TGF-β1 were assessed in three pairs of *Tgfbr1*$^{+/+}$ and *Tgfbr1*$^{+/-}$ MEFs. MEF nuclear extracts were used for Western blot analysis probed with pSmad3 antibodies. Histone 1 is a loading control for nuclear protein extracts. The MEF pair presented is representative of the three pairs of MEFs.

(C) Differential regulation of cell cycle mediators: Western blot analysis of *Tgfbr1*$^{+/+}$ and *Tgfbr1*$^{+/-}$ MEFs in the absence (time 0) and in the presence of 100 pM TGF-β1 for 1, 4, 8, and 16h. The MEF pair presented is representative of the three pairs of MEFs.

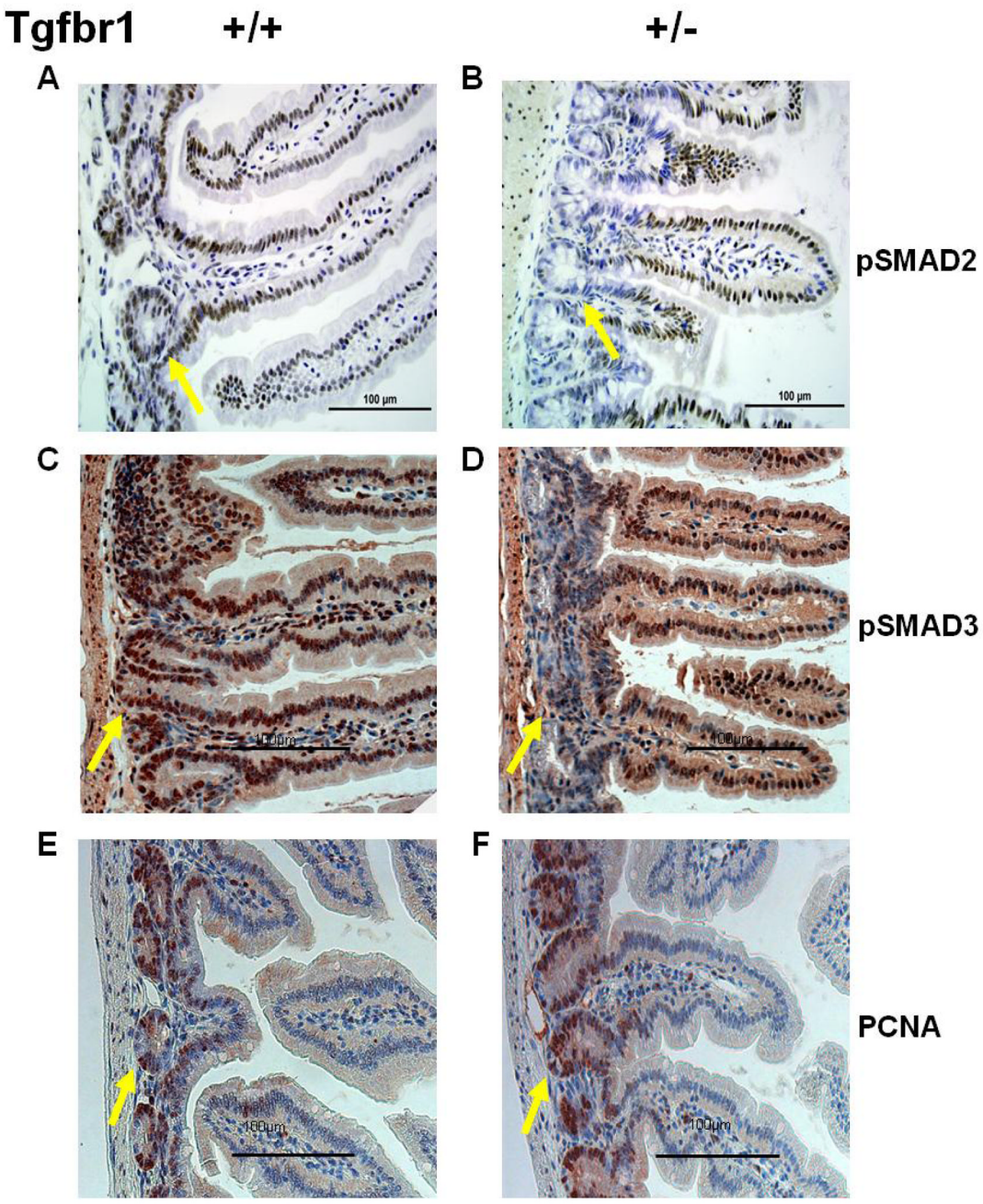

Figure 5. Immunohistochemistry staining patterns of normal appearing small bowel tissues from *Apc*$^{Min/+}$;*Tgfbr1*$^{+/+}$ and *Apc*$^{Min/+}$; *Tgfbr1*$^{+/-}$ mice

(A and B) Normal appearing small intestine stained with pSmad2 shows identical staining pattern throughout the villi of both *Apc*$^{Min/+}$;*Tgfbr1*$^{+/+}$ mice (A) and *Apc*$^{Min/+}$; *Tgfbr1*$^{+/-}$ mice (B). However, pSmad2 staining within the intestinal crypts of *Apc*$^{Min/+}$; *Tgfbr1*$^{+/-}$ mice (arrow) is reduced when compared with that of their wild type counterparts (arrow).

(C and D) Normal appearing small intestine stained with pSmad3 shows identical staining pattern throughout the villi of both *Apc*$^{Min/+}$;*Tgfbr1*$^{+/+}$ mice (C) and *Apc*$^{Min/+}$; *Tgfbr1*$^{+/-}$ mice (D). However, pSmad3 staining within the intestinal crypts of *Apc*$^{Min/+}$; *Tgfbr1*$^{+/-}$ mice (arrow) is reduced when compared with that of their wild type counterparts (arrow).

(E and F) Levels of proliferating cell nuclear antigen (PCNA) expression were significantly higher in $Apc^{Min/+};Tgfbr1^{+/-}$ intestinal epithelial crypts (F, 62.2 ± 2.2% of positive staining) (arrow) than in their wild type counterpart (E, 44.4 ± 2.8% positive staining) (arrow) ($p = 0.008$).

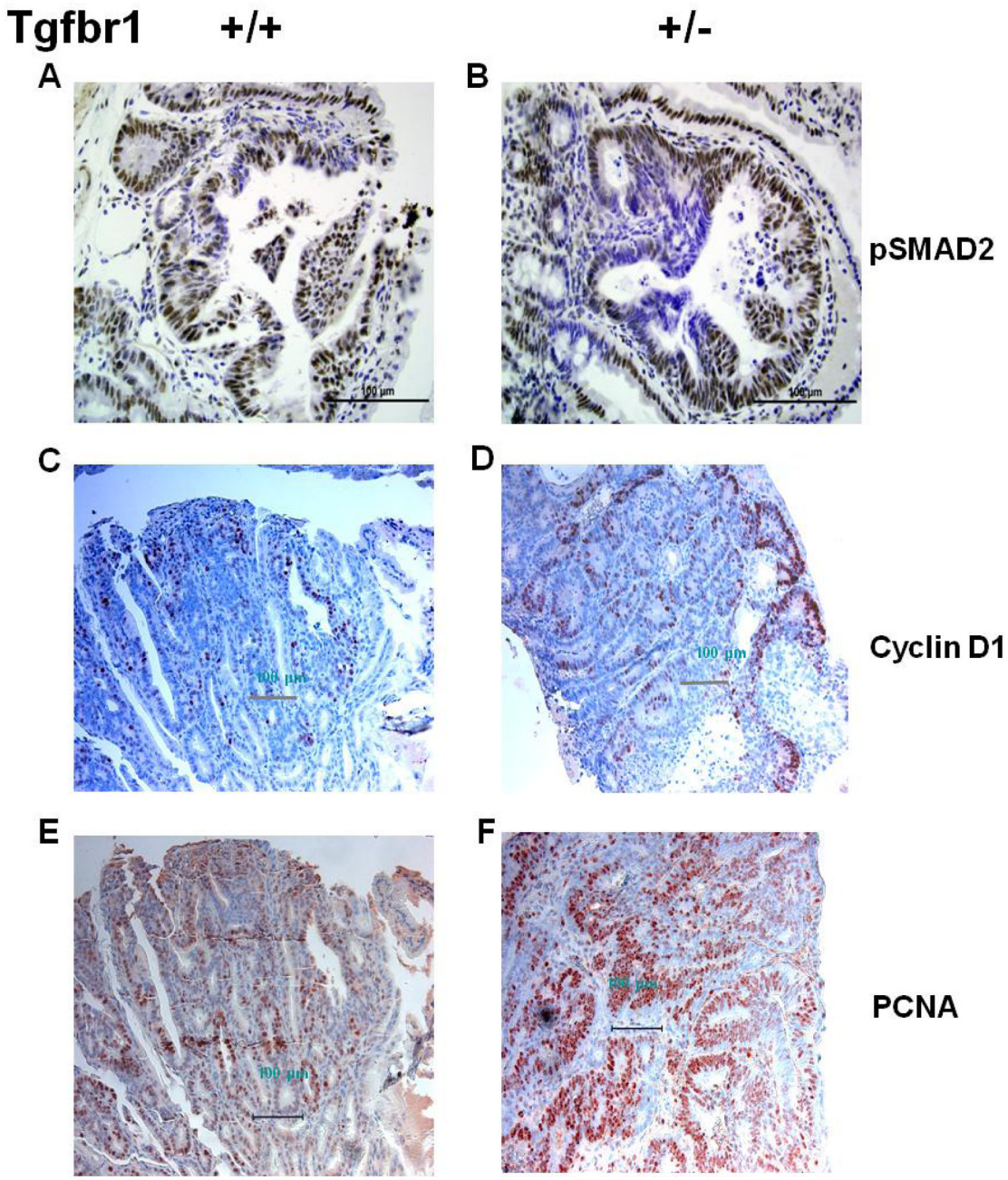

Figure 6. Characterizing the effect of *Tgfbr1* haploinsufficiency on molecular signaling within tumors

(A and B) pSmad2 staining is patchy within tumors arsising from $Apc^{Min/+}$; $Tgfbr1^{+/-}$ mice, which reflects focally-decreased Smad-mediated TGF-β signaling (B), whereas tumors arising from $Apc^{Min/+}$;$Tgfbr1^{+/+}$ mice (B) have uniform pSmad2 staining showing preserved Smad-mediated TGF-β signaling (A).

(C and D) Ccnd1 (cyclin D1) expression is significantly higher in the tumors of $Apc^{Min/+}$; $Tgfbr1^{+/-}$ mice (F, 50.7 ± 4.1% positive staining) than in those of $Apc^{Min/+}$; $Tgfbr1^{+/+}$ mice (E, 20.1 ± 5.7% positive staining), p = 0.002.

(E and F) Levels of proliferating cell nuclear antigen (PCNA) expression are significantly higher in $Apc^{Min/+}$; $Tgfbr1^{+/-}$ tumors (H, 82.0 ± 2.9% of positive staining) than in their wild type counterpart (G, 48.2 ± 3.8% positive staining) ($p = 0.0003$) indicating increased cellular proliferation in vivo.